JPP Journal of Pharmacy and Pharmacology
ROYAL PHARMACEUTICAL SOCIETY

JPP Journal of Pharmacy and Pharmacology

JPP 2011, 63: 1462–1469

Received March 2, 2011
Accepted August 15, 2011
DOI
10.1111/j.2042-7158.2011.01350.x
ISSN 0022-3573

Research Paper

CPUYJ039, a newly synthesized benzimidazole-based compound, is proved to be a novel inducer of apoptosis in HCT116 cells with potent KSP inhibitory activity

Cheng Jiang[a,b,*], Lei Yang[c,*], Wu-Tong Wu[c], Qing-Long Guo[a] and Qi-Dong You[a,b]

[a]Jiangsu Key Laboratory of Carcinogenesis and Intervention, [b]Department of Medicinal Chemistry, [c]School of Life Science and Technology, China Pharmaceutical University, Nanjing, China

Abstract

Objectives This study investigated the antiproliferative and apoptotic activities of CPUYJ039, a newly synthesized benzimidazole-based kinesin spindle protein (KSP) inhibitor, on HCT116 cell lines.

Methods KSP-inhibitory activity was tested using the malachite-green method. The in-vitro cell proliferation inhibitory activity of the sample was measured using WST reagent. Flow-cytometric evaluation of cellular DNA content was performed. Apoptotic cells were quantified by annexin V-FITC-PI double staining. To confirm that the cytotoxic activity was a consequence of KSP inhibition, microtubule morphology and DNA segregation were observed by double staining of microtubules and DNA. The expression of Bcl-2 and Bax in CPUYJ039-treated HCT116 cells was detected by Western blotting.

Key findings CPUYJ039 was evaluated and proved to have potent inhibitory activities in the KSP ATPase and HCT116 cell proliferation assays. CPUYJ039 inhibited the proliferation of HCT116 cells in a dose- and time-dependent manner and markedly induced G2/M phase cell-cycle arrest with characteristic monoastral spindles and subsequent cell death in HCT116 cells, which was associated with an increase of the Bax/Bcl-2 ratio.

Conclusions These results suggest that CPUYJ039 may be a novel inducer of apoptosis in HCT116 cells with potent KSP inhibitory activity.

Keywords antitumor; apoptosis; cell cycle; HCT116 cells; KSP inhibitor

Introduction

Mitosis is a highly regulated process during cell division. Antimitotic agents, such as the vinca alkaloids and the taxanes, interfere with the polymerization–depolymerization process of microtubules and lead to cell cycle arrest in mitosis. However, these agents target microtubules and display several undesirable side effects in non-dividing cells, such as neurotoxicity. Thus, it is necessary to develop antimitotics that do not act on microtubules directly.

Mitotic motor proteins, some of which are kinesins, are required for bipolar spindle formation during mitosis.[1] Several members of the kinesin family play essential roles in mitotic spindle function and are potential targets in novel antimitotic cancer therapeutics. Kinesin spindle protein (KSP), also known as Eg5, is a member of the kinesin superfamily that utilizes the energy generated from the hydrolysis of ATP to transport vesicles, organelles and microtubules. KSP is also required for centrosome separation during prophase or prometaphase.[2]

Inhibition of KSP prevents the formation of normal bipolar spindles, which leads to mitotic arrest with a characteristic monoastral phenotype and subsequently apoptosis in transformed cells, without disturbing the function of microtubules.[3,4] Thus KSP inhibition represents a novel and specific mechanism to target the mitotic spindle, which may be devoid of the neuropathy-associated, mechanism-based side effects common to the taxanes and other natural products that target microtubules.

In recent years, several classes of KSP inhibitors have been reported.[5–21] The pharmacophore identification and binding mode analysis based on the reported KSP inhibitors have been presented in our previous studies.[22,23]

Correspondence: Qi-Dong You, Jiangsu Key Laboratory of Carcinogenesis and Intervention, 24 Tongjiaxiang, Nanjing 210009, China.
E-mail: youqidong@gmail.com

*Dr Cheng Jiang and Lei Yang contributed equally to this paper.

In the literature reported up until now, the lead compounds were usually gained by screen. Thus it is difficult to find novel inhibitors by compound screen. In pursuit of novel KSP inhibitors, we used the drug discovery program LUDI (Accelrys), an automated fragment-based suggestive program for the de-novo design of protein ligands. A benzimidazole-based compound CPUYJ039 was found to exert potent inhibitory activity on KSP. The inhibitory effect of this compound on the growth of human colon carcinoma cell HCT116 was then investigated. In this study, we demonstrated that CPUYJ039 inhibited KSP ATPase activity and induced apoptosis through arresting the cell cycle in the G2/M phase. In addition, the apoptotic pathways induced by CPUYJ039 involved the elevation of the Bax/Bcl-2 ratio. Furthermore, CPUYJ039-treated cells displayed the monastral spindle phenotype, which is typical in KSP inhibition. These results provided a mechanistic framework for further exploration of CPUYJ039 as a novel chemotherapeutic agent for human tumors.

Materials and Methods

Discovery of CPUYJ039

According to the results of our analysis of the binding mode of KSP inhibitors,[23] the site for KSP inhibitors' interaction is composed of two cooperative sub-cavities: a main pocket in which most inhibitors merged and a minor pocket surrounded mainly by Arg221 and Ala218. In the main pocket, the H-bonds formed with Glu116, Glu118 and Tyr211 were determinant and the hydrophobic interactions between the inhibitors and Trp127, Ala133, Tyr211 were especially important. The main binding pocket was essential while the interaction with the 'minor binding pocket' may greatly increase the activity.

Thus, the binding pocket could be divided into three important areas: the area near to Trp127, Ala133 and Tyr211, the area near Glu116 and Glu118, and the area near Arg221 and Ala218.[23] We screened several small fragments that could interact with residues in the binding pocket of KSP by using the LUDI program. The fragment with highest score at each starting point was selected and connected using certain bonds, as shown in Figure 1. The compound shown in structure **1** was obtained.

Modification was then made to compound **1** as shown in Figure 1a. Firstly, the indole core was replaced by benzimidazole for easier synthesis. Then the phenylethyl was replaced by aryl amide for molecule diversity and easier synthesis. The side chains were also modified by taking the compounds in Chiron's patent as a reference.[24] Thus, a benzimidazole-based compound CPUYJ039 was found and evaluated.

Chemicals and reagents

Monastrol (the first-reported small-molecule KSP inhibitor, Figure 1b) and CPUYJ039 (Figure 1a) were chemically synthesized in our group and their structures were identified.

Monastrol was synthesized using the method previously reported by our group.[25] CPUYJ039 was synthesized from readily available starting materials using the optimized synthetic route. The route began with the preparation of 2-propyl benzimidazole from o-phenylenediamine and n-butyric acid. Then atom N^1 of 2-propyl benzimidazole was connected with benzyl using benzyl chloride. After bromization and followed by condensation with *N*,*N*-dimethyl-1,3-propyldiamine, CPUYJ039 was finally obtained after acylation by 4-bromine benzoyl chloride.

CPUYJ039 were dissolved in DMSO to 10 mM and stored at −20°C. Monastrol was treated with the same amount of DMSO as used in the corresponding experiments. The concentrations used here were 8, 12 and 16 μM, and the solutions were freshly diluted with RPMI-1640 (Gibco BRL, NY, USA) to final concentrations. Antibodies of β-actin, p53, Bcl-2 and Bax were from (Santa Cruz, CA, USA). DAPI was from (Santa Cruz, CA, USA). IRDye™800 conjugated secondary antibodies were obtained from Rockland Inc (Philadelphia, PA, USA). MTT [3-(4,5-dimethylthiazol-2-yl)-2,5-diphenytetrazolium bromide] was obtained from Fluka Chemical Corp (Ronkonkoma, NY, USA) and was dissolved

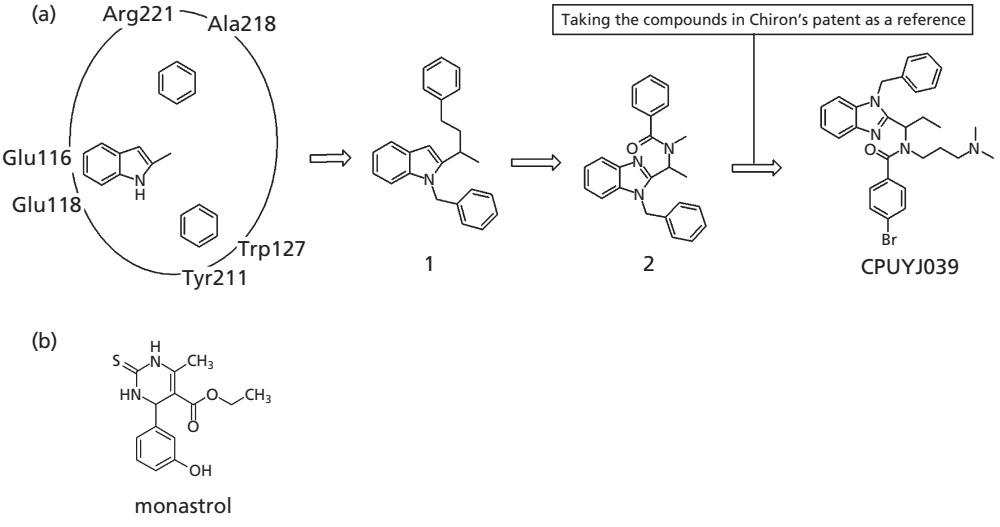

Figure 1 Discovery of CPUYJ039 (a) and chemical structure of monastrol (b).

in 0.01 M PBS. Paclitaxel was obtained from Jiangsu Hengrui Medicine Co., Ltd (Jiangsu, China). All other chemicals were of the highest pure grade available.

Measurement of KSP ATPase activity

The purification of human KSP was described previously.[26] Coding regions were PCR amplified from a template (obtained in our laboratory) containing full-length human KSP. The primers used were forward 50-TATAGG GCG AAT TCC GCC ATG GCG TCG CAG CCA-30 and reverse 50-ACG GGC TGC AGC AAG CTC GAG TTT TAAACG TTC TAT-30. The region encoding residues 2–386 were subcloned into pET28a (NOVAGEN). Protein expression in *Escherichia coli* cells was induced with 0.5 mM IPTG. Cells were harvested after 20 h of growth at 20°C and then disrupted by sonication. The soluble lysate was clarified by centrifugation and applied to a SP-Sepharose column (Amersham Pharmacia Biotech) in a buffer A (20 mM Na-PIPES at pH 6.3, 20 mM NaCl, 1 mM $MgCl_2$, 1 mM Na-EGTA). Protein was eluted with a linear gradient of 20–1000 mM NaCl. KSP was identified by SDS-PAGE and then applied to Mono-Q columns (Amersham Pharmacia Biotech) in a buffer B (20 mM Tris-HCl at pH 8.8. 1 mM $MgCl_2$, 1 mM Na-EGTA). A gradient from 0 to 1000 mM NaCl was used to elute Eg5. Fractions were analysed by SDS-PAGE. The most concentrated fraction was dialysed against ATPase buffer (20 mM Na-PIPES, pH 7.5; 1 mM $MgCl_2$; 1 mM Na-EGTA) and then aliquoted, frozen in liquid nitrogen and stored at −80°C.

Tubulin was purified from bovine brain by two cycles of polymerization–depolymerization as described by Williams and Lee.[27] Tubulin was aliquoted and frozen in liquid nitrogen and stored at −80°C. Before the day of experiment, an aliquot of tubulin was polymerized into microtubules overnight at 37°C at 5 mg/ml in the presence of 20 μM paclitaxel.

All experiments were done at room temperature. The reagents were added to a 96-well clear plate and the final reaction of the assay contained 20 mM PIPES (pH 7.5), 5.0 mM $MgCl_2$, 1 mM EGTA, 10 μM paclitaxel, 0.6 μM tubulin (MT), 0.5 mM ATP and 2% DMSO containing the test compound (this DMSO concentration had no effect on the ATPase activity) in a reaction volume of 100 μl. Reactions were started by adding ATP. The plates were then incubated at 37°C for 30 min. Following incubation a malachite-green based reagent was added to detect the release of inorganic phosphate.[28] The plates were incubated for an additional 5 min at room temperature, and then 10 μl 34% sodium citrate was added. The absorbance at 610 nm was determined using a Multiskan Spectrum Microplate Spectrophotometer (Thermo Electron Corporation). The controls without KSP or MTs are the background and should be subtracted from all values. The controls with MTs but without KSP give the nucleotide hydrolysis by MTs and should be subtracted from corresponding values with KSP and the same concentration of MTs. The data were analysed and the IC50 values were calculated.

Cell culture and proliferation assay

The human colon carcinoma HCT116 cells were grown in RPMI 1640 medium supplemented with 10% fetal calf serum, 100 U/ml penicillin, 100 μg/ml streptomycin and cultured in a humidified atmosphere containing 5% CO_2 at 37°C.

Cells grown in 96-well plates (5×10^3 cells per well) were treated with different concentrations of test compounds for 48 h. The cell proliferation was measured using WST reagent (Quick Cell Proliferation Assay Kit Π). The percentage of cell proliferation as a function of drug concentration was plotted to determine the IC50 value.

Flow cytometry

Flow cytometric evaluation of cellular DNA content was performed as described elsewhere.[29] Briefly, cells were cultured with CPUYJ039 (8 μM, 12 μM, 16 μM) for 24 h or 48 h at 37°C. Then 2×10^6 cells were collected, washed twice with ice-cold phosphate-buffered saline (PBS) and fixed in 70% ethanol at 4°C until further procession. Cells were washed again with PBS and incubated with propidium iodide (PI) (20 μg/ml)/RNase A (20 μg/ml) in PBS for 30 min in the dark. Data acquisition and analysis were performed in a Becton Dickinson FACSCalibur flow cytometer using CellQuest software (BD Biosciences, Franklin Lakes, NJ, USA).

Annexin V/PI staining

Apoptotic cells were quantified by annexin V-FITC-PI double staining, using a kit purchased from Bipec. In brief, cells were incubated with the designated doses of CPUYJ039 for 24 h. Cells were washed twice with cold PBS and then resuspended in 500 μl binding buffer at a concentration of 1×10 cells/ml.[6] Annexin V-FITC and PI were then added according to the manufacturer's instructions. The fluorescence was immediately determined by flow cytometry.

Western blot analysis

The effect of CPUYJ039 treatment on the expression of the Bcl-2 family of anti- (Bcl-2) and pro-apoptotic (Bax) proteins and the p53 protein was determined to gain insight into the mechanism for CPUYJ039-induced cell death. HCT116 cells were incubated with CPUYJ039 at various concentrations for 48 h. Cells were collected and lysed in lysis buffer (50 mM Tris-Cl, pH 7.6, 150 mM NaCl, 1 mM EDTA, 1% (m/v) NP-40, 0.2 mM PMSF, 0.1 mM NaF and 1.0 mM DTT). The lysates were clarified by centrifugation at 4°C for 15 min at 13 000*g*. The protein concentration was determined with the BCA reagent. Equal amounts of protein were subjected to electrophoresis on 10% SDS–polyacrylamide gels and transferred onto the PVDF membranes (Millipore, Boston, MA, USA). The blots were incubated with appropriate primary antibodies overnight at 4°C followed by IRDye™800 conjugated secondary antibody for 1 h at 37°C. Detection was performed by the Odyssey Infrared Imaging System (LI-COR Inc., USA). All blots were stripped and reprobed with polyclonal anti-β-actin antibody to ascertain equal loading of proteins. The intensity of each band was measured using GELPro 4.0 software. The ratio of the integrated optical densities of Bax/Bcl-2 was calculated.

Immunofluorescence microscopy

The HCT116 cells were left to adhere for at least 12 h on poly-(D-lysine)-coated glass coverslips before the addition of CPUYJ039 (8 μM). Following incubation with drug for 20 h, cells were fixed with 4% paraformaldehyde–PBS at 37°C for 45 min, washed with PBS for 5 min twice, permeabilized with

0.2% TX100 in PBS for 30 min at 4°C, and washed with PBS for 5 min. Then cells were incubated with 3% bovine serum albumin–PBS for 1 h at room temperature, followed by staining with anti-β-tubulin antibody (Santa Cruze) for 12 h at 4°C, washing with PBS for 5 min, then processing with an FITC-conjugated goat anti-rat secondary antibody (Santa Cruze) for 1 h at room temperature and counterstaining with PI. Images were collected with a Leica™ Fluorescence microscope equipped with a Leica™ camera.

Statistical analysis

All data were expressed as mean ± standard deviation (SD). The effect of concentration on KSP or cell viability was analysed using a Kruskal–Wallis test. Individual differences between the concentrations were evaluated using Dunn's test. The difference between 24-h and 48-h treatments at each concentration was assessed using a Mann Whitney U test. The difference between CPUYJ039 and monastrol treatment was analysed using a Mann Whitney U test. A value of $P < 0.05$ was considered significant.

Results

CPUYJ039 inhibited the microtubule-stimulated ATPase activity of KSP and exhibited potent growth inhibition in HCT116 cells

The IC50 value of CPUYJ039 against KSP was 0.04 μM, while that of monastrol was 7.45 μM (Figure 2a). CPUYJ039 also showed potent growth-inhibitory activities against HCT116 cells in a dose-dependent manner, with an IC50 value of 2.30 μM, while it was more than 10 μM for monastrol (Figure 2b).

CPUYJ039 induces G2/M phase cell cycle arrest

As shown in Figure 3a, DNA flow cytometric analysis indicated a dose-dependent accumulation of cells at the G2/M phase, which was seen as early as 24 h after treatment (from 12% to 40%). This G2/M accumulation was strengthened (from 12% to 72%) following 48-h treatment and induced a profound sub-G0 peak at the higher doses (12 and 16 μM).

Effect of CPUYJ039 on cell morphology

Microtubule morphology and DNA segregation were observed by double staining of microtubules and DNA (Figure 3b). Untreated control cells showed a typical bipolar mitotic spindle. In contrast, CPUYJ039-treated cells showed a monoastral microtubule array that was surrounded by a ring of chromosomes.

CPUYJ039-induced cell death via apoptosis

To further confirm the apoptotic effect induced by CPUYJ039, flow cytometry with the fluorescein isothiocyanate annexin V/PI double staining assay was carried out. As shown in Figure 4a, after treatment with 8, 12 and 16 μM CPUYJ039 for 24 h, the early and median apoptotic cells (right lower section of fluorocytogram) were increased (from 0.4% to 14.5%, 16.3% and 25.5%, respectively) and the late apoptotic and necrotic cells (right upper section of fluorocytogram) were also increased strikingly (from 0.1% to 2.3%, 4.2% and 2.4%).

Effects of CPUYJ039 on apoptotic signaling pathway

The balance of anti-apoptotic and pro-apoptotic Bcl-2 family members largely determines the susceptibility of cells to apoptotic signals. Thus we further detected the protein expression of Bcl-2 and Bax, and found that the levels of Bcl-2 was decreased while Bax was increased, leading to a rise in the Bax/Bcl-2 ratio (Figure 4b and 4c). In the meantime, we found that the expression of another apoptosis-related protein, p53, was hardly affected in CPUYJ039-treated cells (Figure 4b).

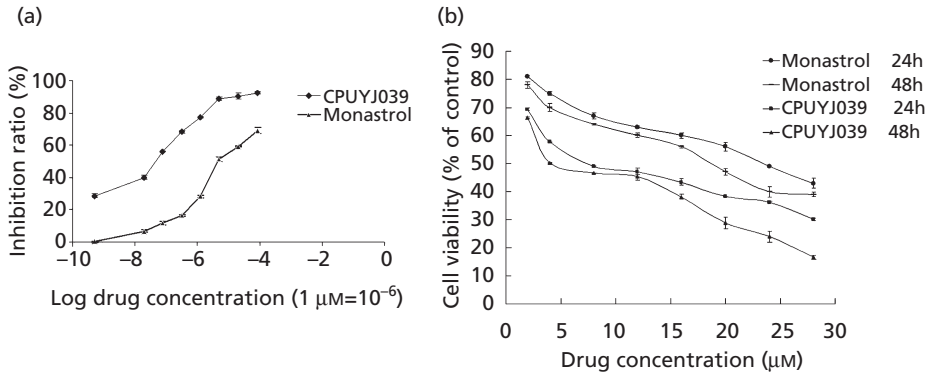

Figure 2 (a) In-vitro KSP inhibitory activity of monastrol and CPUYJ039. The data are expressed as an inhibition ratio and represent the mean ± SEM of three independent experiments. The effect of concentration on KSP inhibition was significant ($P < 0.05$). Individual differences between the concentrations were significant ($P < 0.05$). Treatment with CPUYJ039 resulted in a significant increase in KSP inhibition compared with the monastrol-treated group ($P < 0.05$). (b) Effect of monastrol and CPUYJ039 on the proliferation of HCT116 cells. Cells were treated with different concentrations of monastrol and CPUYJ039 for 24 and 48 h, respectively, and cell proliferation was determined by using the WST assay. The data are expressed as a percentage of the control (100%) and represent the mean ± SEM of three independent experiments. The effect of concentration on cell viability was significant ($P < 0.05$). Individual differences between the concentrations were significant ($P < 0.05$). Treatment with CPUYJ039 resulted in a significant decrease in cell viability compared with the monastrol-treated group ($P < 0.05$). Differences between 24 h and 48h-treatments were statistically significant at the concentrations 20, 24 and 28 μM ($P < 0.05$).

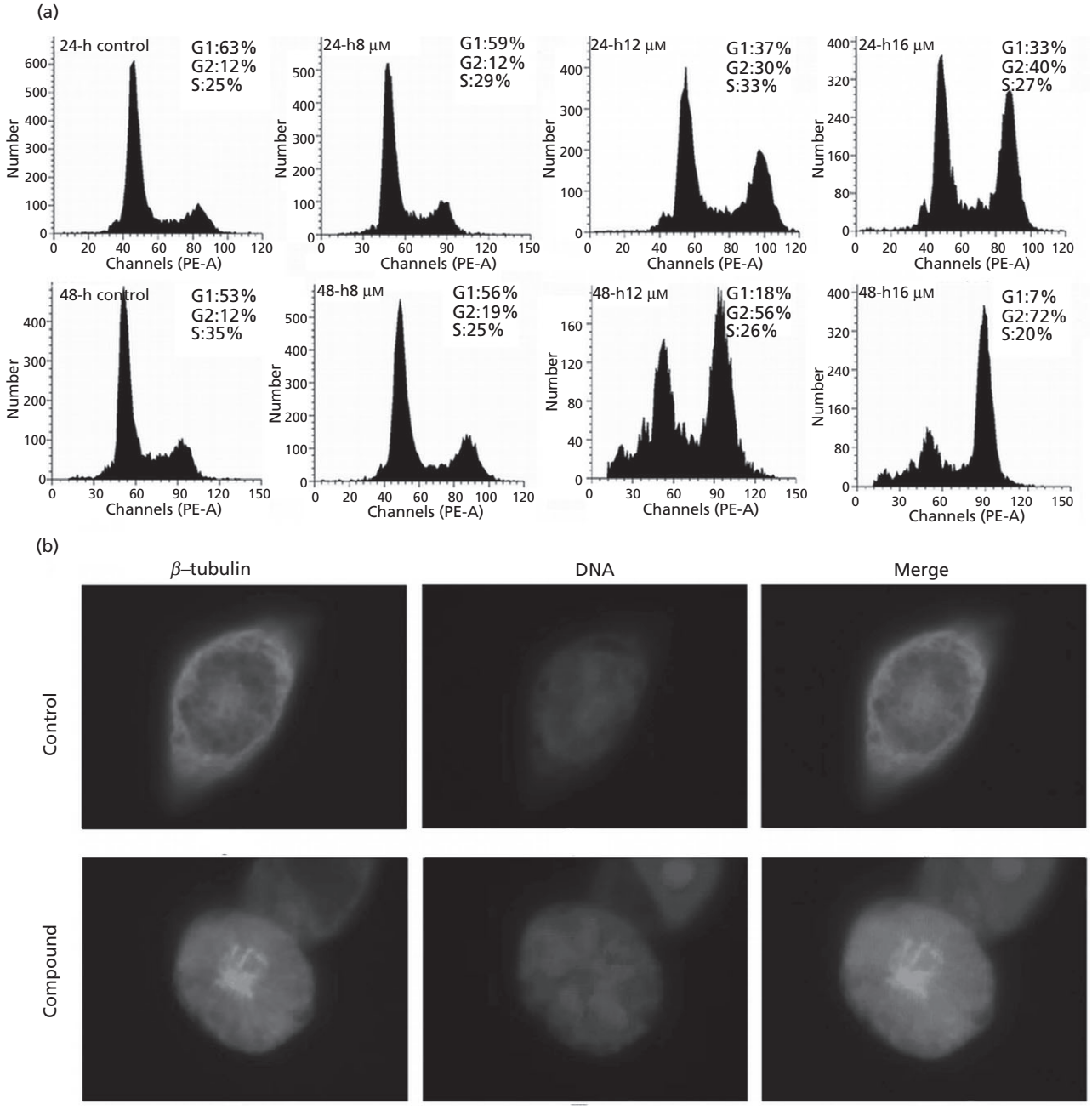

Figure 3 Effects of CPUYJ039 on the cell cycle distribution and the cell morphology in HCT116 cells. (a) Treatment of HCT116 cells with CPUYJ039 led to profound G2/M arrest. Cells were treated with the compound (8, 12 or 16 μM) for 24 or 48 h. Control cells were treated with DMSO alone. (b) CPUYJ039 affected spindle formation. HCT116 cells were treated in the absence or presence of CPUYJ039 (16 μM) for 24 h, and β-tubulin (green) and DNA (red) of cells were immunofluorescence stained. The merge images of them are also shown. Normal bipolar spindles and DNA alignment at metaphase plate of control cells were replaced with a mono-astral spindle surrounded by chromosomes in CPUYJ039-treated cells (magnification 630*).

Discussion

In this study, CPUYJ039 was selected to investigate its biological activity. Firstly, KSP inhibitory activities were tested using the malachite-green method. The IC50 value of CPUYJ039 against KSP was 0.04 μM, making it about 186-fold more potent than monastrol (IC50 = 7.45 μM). This result suggests CPUYJ039 is a potent KSP inhibitor. Then the in-vitro cytotoxicities of the samples were tested. CPUYJ039 showed potent inhibitory activities against HCT116 cells with an IC50 value of 2.30 μM, while the figure was more than 10 μM for monastrol. The results indicate that CPUYJ039 inhibits the proliferation of HCT116 cells in a dose-dependent manner. Moreover, CPUYJ039 also displayed inhibitory effects on the growth rate of some other cancer cells, such as human lung cancer A549 cells, human gastric cancer AGS

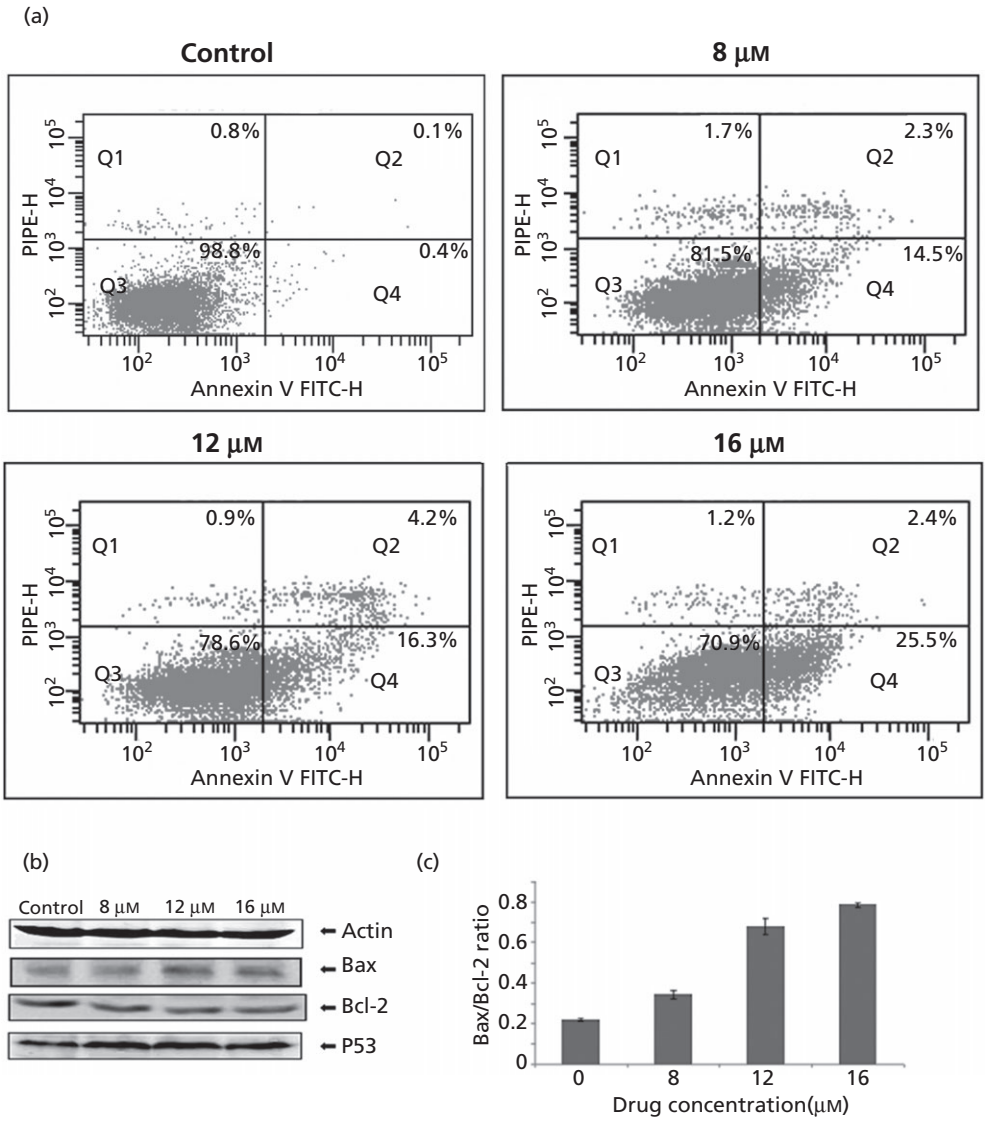

Figure 4 The apoptotic effects of CPUYJ039 in human colon carcinoma HCT116 cells. (a) Induction of apoptosis, measured by Annexin V assay following treatment with CPUYJ039 (8 to 16 μM) for 24 h. Control cells were treated with DMSO alone. (b) Effect on Bcl-2 family and p53 in HCT116 cells after treatment with different concentrations of CPUYJ039 (8 to 16 μM) for 48 h. Total cell lysates were prepared and immunoblotted. Western blots were detected with antibodies against Bax, Bcl-2, p53 and β-actin. (c) The Bax/Bcl-2 ratio in Western blot analysis. Bax/Bcl-2 ratio was measured by densitometric analysis after normalising the bands to that of β-actin. Treatment with CPUYJ039 resulted in a significant increase in Bax/Bcl-2 ratio ($P < 0.05$, KruskalWallis).

cells and human hepatocellular carcinoma HepG2 cells (data not shown), which indicates that CPUYJ039 possesses a broad spectrum of activity against human cancer cells. When the highly potency of the KSP inhibition is considered, the antiproliferative activity of CPUYJ039 was significantly low. This may be caused by the low cell permeation of this compound. Mechanistic studies need to be carried out to further understand the cause of this phenomenon.

Suppression of cell growth by CPUYJ039 can be explained by cell cycle arrest. Cell cycle analysis revealed that inhibition of cell viability by CPUYJ039 results from cell cycle arrest at the G2/M phase, accompanied by an increase in the sub-G0 fraction, indicating apoptotic cell death. Cell cycle analysis revealed that CPUYJ039 induces cell cycle arrest at the G2/M phase.

To further confirm the apoptotic effect induced by CPUYJ039, flow cytometry with the fluorescein isothiocyanate Annexin V/PI double staining assay was carried out. As shown in Figure 4a, after treatment with 8, 12 and 16 μM CPUYJ039 for 24 h, the early and median apoptotic cells (right lower section of fluorocytogram) were increased (from 0.4% to 14.5%, 16.3% and 25.5%, respectively) and the late apoptotic and necrotic cells (right upper section of fluorocytogram) were also increased significantly (from 0.1% to 2.3%, 4.2% and 2.4%). These results demonstrate that CPUYJ039 induces cell death mainly via apoptosis and in a dose-dependent manner.

To confirm that the cytotoxic activity was a consequence of KSP inhibition, we further characterized the cellular activity of CPUYJ039. As shown in Figure 3b, incubation with CPUYJ039 caused mitotic arrest in HCT116 cells by inducing the formation of monoasters (a rosette of condensed mitotic chromosomes), which is typical for KSP inhibition. These indicate that during the onset of mitosis, the duplicated centrosomes fail to fully separate to form the bipolar mitotic spindle and remain locked with a monoastral spindle phenotype.

The Bcl-2 family members are key regulators of apoptosis and are overexpressed in many malignancies. The up-regulation of Bcl-2 protects cells from apoptosis, whereas cells with increased Bax expression undergo apoptosis by suppressing Bcl-2 activity. The expression of Bcl-2 and Bax in CPUYJ039-treated HCT116 cells were detected by Western blotting. It was showed that the expression of Bcl-2 was strikingly decreased and that of Bax was increased in CPUYJ039-treated HCT116 cells, which led to an increase of the Bax/Bcl-2 ratio. This showed that CPUYJ039 could be an effective apoptosis inducer in HCT116 cells.

Conclusions

Based on all those results, we come to a conclusion that CPUYJ039 may be a novel inducer of apoptosis in HCT116 cells with potent KSP inhibitory activity. CPUYJ039-treated HCT116 cells were led to mitotic arrest with the formation of monoastral spindles and subsequent cell death. Detailed mechanistic studies need to be carried out to further understand the antitumor mechanism of this newly synthesized compound.

Declarations

Conflict of interest

The Author(s) declare(s) that they have no conflicts of interest to disclose.

Funding

This work was financially supported by a grant from 'The Six Top Talents' of Jiangsu Province (no. 06-C-023), Specialized Research Fund for the Doctoral Program of Higher Education PRC (no. 20060316006) and National Natural Science Foundation (no. 30772624 and no. 30801437). This work was also financially supported by Jiangsu Hengrui Medicine Co., Ltd.

References

1. Heald R. Motor function in the mitotic spindle. *Cell* 2000; 102: 399–402.
2. Blangy A *et al*. Phosphorylation by p34cdc2 regulates spindle association of human Eg5, a kinesin-related motor essential for bipolar spindle formation in vivo. *Cell* 1995; 83: 1159–1169.
3. Sharp DJ *et al*. Microtubule motors in mitosis. *Nature* 2000; 407: 41–47.
4. Mayer TU *et al*. Small molecule inhibitor of spindle bipolarity identified in a phenotype-based screen. *Science* 1999; 286: 971–974.
5. Nakazawa J *et al*. A novel action of terpendole E on the motor activity of mitotic kinesin Eg5. *Chem Biol* 2003; 10: 131–137.
6. Debonis S *et al*. In vitro screening for inhibitors of the human mitotic kinesin Eg5 with antimitotic and antitumor activities. *Mol Cancer Ther* 2004; 3: 1079–1090.
7. Hotha S *et al*. HR22C16: a potent small-molecule probe for the dynamics of cell division. *Angew Chem Int Ed Engl* 2003; 42: 2379–2382.
8. Sakowicz R *et al*. Antitumor activity of a kinesin inhibitor. *Cancer Res* 2004; 64: 3276–3280.
9. Cox CD *et al*. Kinesin spindle protein (KSP) inhibitors. Part 1: the discovery of 3,5-diaryl-4,5-dihydropyrazoles as potent and selective inhibitors of the mitotic kinesin KSP. *Bioorg Med Chem Lett* 2005; 15: 2041–2045.
10. Fraley ME *et al*. Kinesin spindle protein (KSP) inhibitors. Part 2: the design, synthesis, and characterization of 2,4-diaryl-2,5-dihydropyrrole inhibitors of the mitotic kinesin KSP. *Bioorg Med Chem Lett* 2006; 16: 1775–1779.
11. Garbaccio RM *et al*. Kinesin spindle protein (KSP) inhibitors. Part 3: synthesis and evaluation of phenolic 2,4-diaryl-2,5-dihydropyrroles with reduced hERG binding and employment of a phosphate prodrug strategy for aqueous solubility. *Bioorg Med Chem Lett* 2006; 16: 1780–1783.
12. Cox CD *et al*. Kinesin spindle protein (KSP) inhibitors. Part 4: structure-based design of 5-alkylamino-3,5-diaryl-4,5-dihydropyrazoles as potent, water-soluble inhibitors of the mitotic kinesin KSP. *Bioorg Med Chem Lett* 2006; 16: 3175–3179.
13. Kim KS *et al*. Synthesis and SAR of pyrrolotriazine-4-one based Eg5 inhibitors. *Bioorg Med Chem Lett* 2006; 16: 3937–3942.
14. Tarby CM *et al*. Inhibitors of human mitotic kinesin Eg5: characterization of the 4-phenyl-tetrahydroisoquinoline lead series. *Bioorg Med Chem Lett* 2006; 16: 2095–2100.
15. Cox CD *et al*. Kinesin spindle protein (KSP) inhibitors. Part V: discovery of 2-propylamino-2,4-diaryl-2,5-dihydropyrroles as potent, water-soluble KSP inhibitors, and modulation of their basicity by beta-fluorination to overcome cellular efflux by P-glycoprotein. *Bioorg Med Chem Lett* 2007; 17: 2697–2702.
16. Coleman PJ *et al*. Kinesin spindle protein (KSP) inhibitors. Part 6: design and synthesis of 3,5-diaryl-4,5-dihydropyrazole amides as potent inhibitors of the mitotic kinesin KSP. *Bioorg Med Chem Lett* 2007; 17: 5390–5395.
17. Garbaccio RM *et al*. Kinesin spindle protein (KSP) inhibitors. Part 7: design and synthesis of 3,3-disubstituted dihydropyrazolobenzoxazines as potent inhibitors of the mitotic kinesin KSP. *Bioorg Med Chem Lett* 2007; 17: 5671–5676.
18. Roecker AJ *et al*. Kinesin spindle protein (KSP) inhibitors. Part 8: design and synthesis of 1,4-diaryl-4,5-dihydropyrazoles as potent inhibitors of the mitotic kinesin KSP. *Bioorg Med Chem Lett* 2007; 17: 5677–5682.
19. Pinkerton AB *et al*. Synthesis and SAR of thiophene containing kinesin spindle protein (KSP) inhibitors. *Bioorg Med Chem Lett* 2007; 17: 3562–3569.
20. Parrish CA *et al*. Novel ATP-competitive kinesin spindle protein inhibitors. *J Med Chem* 2007; 50: 4939–4952.
21. Jiang C *et al*. Kinesin spindle protein Inhibitors as anticancer agents. *Expert Opin Ther Patents* 2006; 16: 1517–1532.
22. Liu F *et al*. Pharmacophore identification of KSP inhibitors. *Bioorg Med Chem Lett* 2007; 17: 722–726.
23. Jiang C *et al*. Docking studies on kinesin spindle protein inhibitors: an important cooperative 'minor binding pocket' which increases the binding affinity significantly. *J Mol Model* 2007; 13: 987–992.
24. Boyce RS *et al*. Indole and benzimidazole derivatives. WO2006049835; 2006.

25. Jiang C *et al*. An efficient and solvent-free one-pot synthesis of dihydropyridinones under microwave irradiation. *Chin Chem Lett* 2007; 18: 647–650.
26. Yang L *et al*. Cloning, enzyme characterization of recombinant human Eg5 and the development of a new inhibitor. *Biol Pharm Bull* 2008; 31: 1397–1402.
27. Williams RC Jr, Lee JC. Preparation of tubulin from brain. *Methods Enzymol* 1982; 85: 376–385.
28. Ohno T, Kodama T. Kinetics of adenosine triphosphate hydrolysis by shortening myofibrils from rabbit psoas muscle. *J Physiol* 1991; 441: 685–702.
29. Han YW *et al*. The changes of intracellular H(2)O(2) are an important factor maintaining mitochondria membrane potential of antimycin A-treated As4.1 juxtaglomerular cells. *Biochem Pharmacol* 2007; 73: 863–872.